Princeton Optronics

is now

Member of the ams Group

The technical content of this Princeton Optronics document is still valid.

Contact information:

Headquarters:
ams AG
Tobelbader Strasse 30
8141 Premstaetten, Austria
Tel: +43 (0) 3136 500 0
e-Mail: ams_sales@ams.com

Please visit our website at www.ams.com

High-power red VCSEL arrays

Jean-Francois Seurin*, Viktor Khalfin, Guoyang Xu, Alexander Miglo, Daizong Li, Delai Zhou, Mukta Sundaresh, Wei-Xiong Zou, Chien-Yao Lu, James D. Wynn, and Chuni Ghosh
Princeton Optronics, 1 Electronics Drive, Mercerville, NJ, USA 08619

ABSTRACT

High-power red laser sources are used in many applications such as cosmetics, cancer photodynamic therapy, and DNA sequencing in the medical field, laser-based RGB projection display, and bar-code scanning to name a few. Vertical-cavity surface-emitting lasers (VCSELs) can be used as high-power laser sources, as efficient single devices can be configured into high-power two-dimensional arrays and scaled into modules of arrays. VCSELs emit in a circular, uniform beam which can greatly reduce the complexity and cost of optics. Other advantages include a narrow and stable emission spectrum, low speckle of the far-field emission, and good reliability. However, developing efficient red VCSEL sources presents some challenges because of the reduced quantum-well carrier confinement and the increased Aluminum content (to avoid absorption) which increases thermal impedance, and also decreases the DBR index contrast resulting in increased penetration length and cavity losses. We have recently developed VCSEL devices lasing in the visible 6xx nm wavelength band, and reaching 30% power conversion efficiency. We fabricated high-power 2D arrays by removing the GaAs substrate entirely and soldered the chips on high thermal conductivity submounts. Such arrays have demonstrated several Watts of output power at room temperature, in continuous-wave (CW) operation. Several tens of Watts are obtained in QCW operation. Results and challenges of these high-power visible VCSEL arrays will be discussed. .

Keywords: Semiconductor laser, 2D array, VCSEL, red laser, visible laser, high power laser, photodynamic therapy, gene sequencing, projection display, bar-code scanning.

1. INTRODUCTION

Laser radiation in the 630~700nm spectral region can be obtained using semiconductor lasers in the material systems AlGaAs and AlGaInP grown on GaAs substrate. Laser generation was obtained at ~685nm using an AlGaAs active region, however this wavelength is on the short end of possible range using AlGaAs active and performance of AlGaAs lasers with wavelength shorter than ~700 nm is unsatisfactory. Following the first successful room temperature operation of an AlGaInP laser in 1983 [1], all practical red semiconductor lasers were produced on AlGaInP.

High power red semiconductor lasers can be used in the same applications originally targeted by red gas and solid state lasers. Potential mass applications include laser pointers, bar code readers, transmitters in optical communication systems, information storage on DVD discs for reading and writing, laser printing and in optical mice. The main demands in these applications are low cost, compactness and high reliability – areas in which the VCSEL technology excels.

High power applications of these lasers also include pumping of optical fiber amplifiers [2] and optical pumping of solid state lasers [3]. In these applications broad area and ridge waveguide lasers were used. High power broad area lasers with high reliability were reported in Ref. [4].These lasers may be used in photodynamic therapy and in displays. High power and good beam quality were achieved in the tapered devices (Ref. [5] and references therein). With an external Bragg grating for the wavelength stabilization these lasers produced a single frequency narrow line-width beam. These lasers are especially appropriate for nonlinear frequency conversion, projection TV and displays, free space optical communication and material processing. They also can be used for the photodynamic therapy. There are a number of research efforts on the influence of red laser radiation on the healing of wounds, both on animals and humans, supporting effectiveness of this therapy [6,7]. Red lasers are also used for cosmetic procedures, such as the healing of acne. Red lasers are also used for tissue imaging, for DNA cleavage and analysis. Another medical application is the investigation of different biochemical processes, by observation of specific fluorescence under red laser illumination.

* jfseurin@princetonoptronics.com; phone: 1 (609) 584-9696; fax: 1 (609) 584-2448; www.princetonoptronics.com

Vertical-Cavity Surface-Emitting Lasers XVII, edited by Kent D. Choquette, James K. Guenter,
Proc. of SPIE Vol. 8639, 86390O · © 2013 SPIE · CCC code: 0277-786X/13/$18
doi: 10.1117/12.2004896

A very important application for red semiconductor lasers is short range optical communications with the use of polymer optical fibers. These fibers have one absorption minimum near the 650nm wavelength. Multi-element, individually addressable VCSEL arrays are a transmitter of choice for high capacity local network. Good reliability and possibility of high speed modulation in the many GHz range (25 GHz intrinsic modulation bandwidth) were demonstrated [8].

Second harmonic generation of ~100mW in the UV region with wavelength around 330nm was demonstrated with AlGaInP VECSEL with external optical pumping [9].

The first demonstration of red VCSELs was done in 1992 (optical pumping) and 1993 (electrical pumping) at Sandia National Laboratories [10,11] and Chiao Tung University in Taiwan [12]. These first VCSEL worked in pulsed regime. Still they contained all the important elements of contemporary red VCSELs: strained InGaP quantum well as active region, AlGaInP barriers and cladding layers, and AlGaAs distributed Bragg reflectors (DBR). The main directions of development work were the fine tuning of the active region structure, improving the quality of the epi material, decreasing DBR resistance with interface grading and doping (see for example Ref. [13], Chap. 7, and Ref. [14], Chap. 12). Electrical and thermal resistances are very important issues for the AlGaInP material system due to low band offset between quantum well and cladding and the resulting increase electron leakage. Severity of these issues increase with shortening of the wavelength so most efforts were for the lasers with wavelength between 650 and 700nm. Introduction of the selective oxidation process to create a conducting aperture in lieu of proton implantation contributed to a significant improvement in performance [15]. As a result of various optimizations, the shortest (pulsed) wavelength of 629nm [16] and threshold current density as low as 1.8kA/cm^2 with output power up to 4.6mW at 650~657nm [17] were demonstrated. With optimization of growth condition and using linear graded C-doped AlGaAs DBRs 5mW CW was demonstrated at 670nm, as well as a maximum lasing temperature of 160 deg C under pulse conditions, at 660nm [18,19]. Temperature characteristics of red VCSELs were investigated in Ref. [20]: a CW power of 0.2mW was obtained at 652nm and 50C. Reliability of red VCSEL was investigated at great length in Ref. [21]. The general conclusion is that 665nm VCSELs can be used under CW up to 60 deg C, and in pulsed up to 85 deg C while maintaining adequate reliability for practical usages. High reliable red VCSELs were also demonstrated in Ref. [22]. A recent review [23] also confirmed the good reliability of red VCSELs.

Some novel approaches in the area of red VCSEL development include the use of photonic crystals to improve single-mode operation [24], as well as the use of InP quantum dots to reduce the threshold current and improve the temperature characteristics [25].

Finally, in terms of high power, optically pumped red VECSEL structures producing more than 1.2W in CW operation (used for the second harmonic generation of UV light) was demonstrated [26,27]. A multi-quantum-well structure with 20 GaInP compressively strained wells was used, with an intra-cavity diamond heat-spreader.

To the best of our knowledge, there are no reports on high-power (Watt-level) electrically-injected red VCSEL sources. It was shown [28,29] that VCSELs can be used as very high-power laser sources by fabricating large two-dimensional (2D) planar arrays of low-power, high-efficiency single-emitters. Power levels can range from a few Watts to several hundred Watts, while keeping the power conversion efficiency (PCE) at high levels (typically >40% for arrays emitting at 808nm or 976nm). These high-power, high-efficiency VCSEL sources preserve many of the advantages present in a single VCSEL device, such as low-cost manufacturing, high reliability, and operation at high temperatures. In addition, such high-power VCSEL arrays emit in a spectrally narrow beam (full-width at half-maximum typically <2nm) and in an intrinsically circular, narrow divergence uniform beam (numerical aperture typically between 0.15 and 0.20) without the need for optics. As such, VCSEL arrays offer much potential for many high-power applications (see Ref. [14], Chap. 8 for example).

In this paper we present recent results on VCSELs emitting at the 650nm and 688nm emission wavelengths. First, we briefly review the red VCSEL single device structure and results. We then discuss the array fabrication process, as it presents some additional challenges compared to a 976nm VCSEL structure for example. We then present results on high-power red VCSEL arrays, and discuss some of the challenges in obtaining high-power CW operation. Finally, a short summary concludes this paper.

2. SINGLE DEVICE DESIGN AND RESULTS

The basic building blocks of VCSEL-based high-power 2D VCSEL arrays are single devices. Depending on the power level required, the high power arrays we developed at various IR wavelengths range from ~1mm x 1mm to ~6mm x 6mm in size and contain from a few hundred to a few 10,000's of elements connected in parallel. VCSEL-based modules can contain single or multiple arrays, depending on the power level required and the application.

Epitaxial VCSEL materials designed to lase around 650nm and 688nm were grown on 10-deg-off N-type GaAs substrate using MOCVD. For current and optical confinement, the selective oxidation process is used to create an aperture near the active region to improve performance. In the case of the 6xx nm material, the growth starts with an etch-stop layer to facilitate substrate removal for processing of arrays as explained below. Following the etch-stop layer is a highly doped N-GaAs layer that is used for the N-contact of the arrays. Then, an AlGaAs N-type high-reflectivity distributed Bragg reflector (DBR) follows. The (AlGa)InP cavity consists of InGaP/(AlGa)InP quantum wells, and is followed by a P-type AlGaAs DBR output mirror, whose reflectivity is optimized for maximum power conversion efficiency (PCE). A high-Aluminum content layer is placed near the first pair of the P-DBR to later form the oxide aperture. The placement and design of the aperture is critical to minimize optical losses and current spreading. Band-gap engineering (including modulation doping) is used to design low-resistivity DBRs with low-absorption losses. A schematic of the structure is shown in Fig. 1.

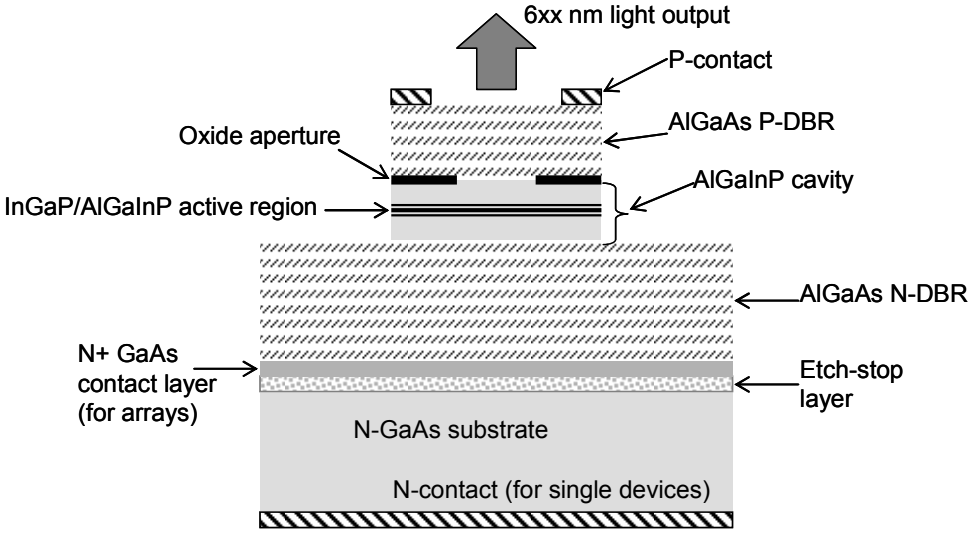

Fig. 1. Schematic of the selectively oxidized, top-emitting 6xx nm VCSEL structure.

The processing of top-emitting single devices is straightforward. On the epitaxial side, Ti/Pt/Au ring contacts of different dimensions are evaporated to form the P-type contacts, which at the same time help act as the self-aligned mask for subsequent dry-etching (RIE) of mesas, deep enough to expose the Aluminum-rich layer. The samples are then exposed to high humidity in a furnace (390~420 deg C) for the selective oxidation process. On the substrate side, Ge/Au/Ni/Au metals are evaporated to form the N-contact. The devices are then probe tested at the wafer level.

Results for single devices operating under CW at a heat-sink temperature of 20 deg C are shown in Fig. 1(a) and (b) for emission wavelengths of 650nm and 688nm, respectively.

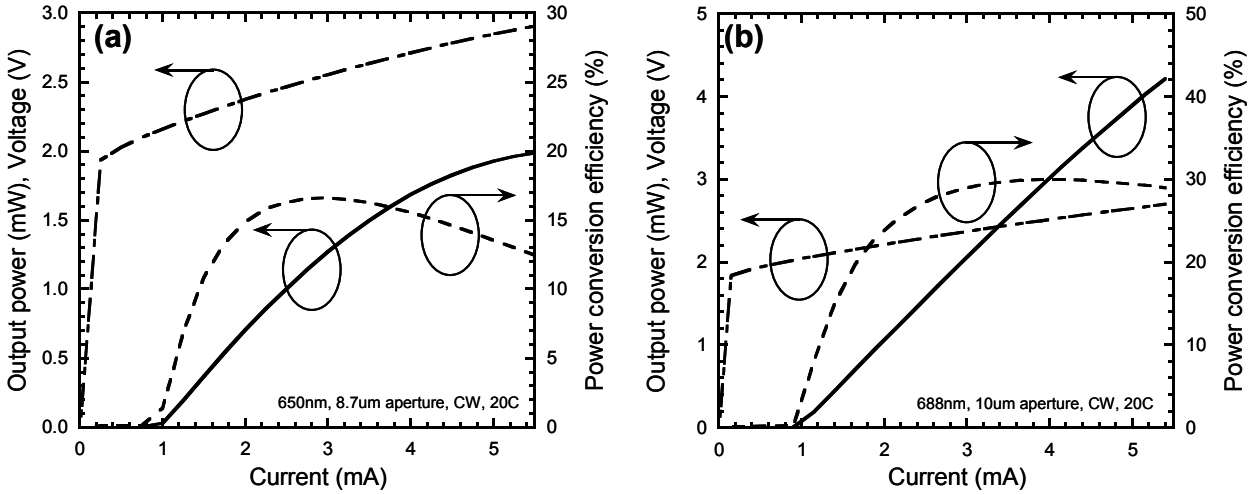

Fig. 2. Output power, voltage, and power conversion efficiency versus drive current for top-emitting single VCSEL devices emitting at (a) 650nm and (b) 688nm. The devices are operated under CW at a 20 deg C heat-sink temperature. The 650nm VCSEL device has an 8.7micron aperture size. The 688nm VCSEL device has a 10micron aperture size.

The 650nm VCSEL device has an 8.7micron aperture size. Threshold current, differential slope efficiency, and differential resistance are 0.96mA, 36%, and 187Ω, respectively. The device reaches a peak power conversion efficiency of ~17% at 3mA current and 1.3mW output power. In terms of efficiency these results are similar to the ones presented in Ref. [17]. The 688nm VCSEL device has a 10micron aperture size. Threshold current, differential slope efficiency, and differential resistance for this device are 0.95mA, 57%, and 155Ω, respectively. The device reaches a peak power conversion efficiency of ~30% at 4mA current and 3mW output power.

The following results (Figure 3) shows the peak power conversion efficiency as a function of aperture size for the 650nm and 688nm emission wavelengths, for devices operated CW at a 20 deg C heat-sink temperature.

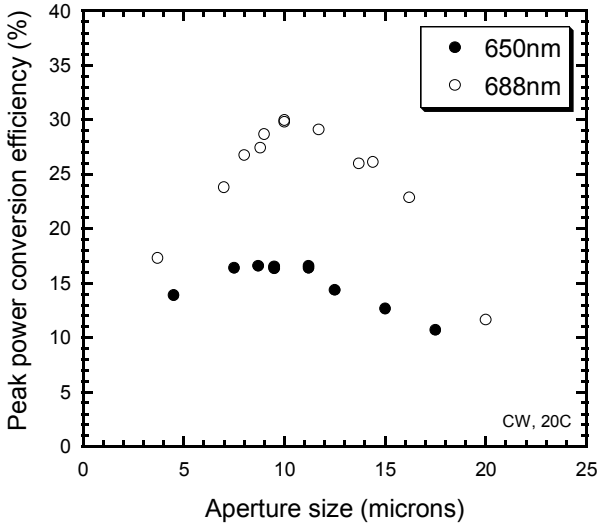

Fig. 3. Peak power conversion efficiency as a function of aperture size for the 650nm and 688nm emission wavelengths, for devices operated CW at a 20 deg C heat-sink temperature.

As can be seen the power conversion efficiency falls off rapidly with increasing aperture size. This is in sharp contrast to the behavior at longer emission wavelengths such as 808nm [29] and 976nm [28]. As mentioned earlier, red

VCSELs face some challenges in terms of high temperature performance because of the higher electron leakage issue and the overall higher Aluminum content in the device, which reduces its thermal conductivity and increase absorption losses. And since the thermal impedance of single VCSEL devices scales as the inverse of the aperture size rather than the aperture area (see Ref. [30], Chap. 2 for example], larger devices will effectively perform worse than small devices. This effect was shown in Ref. [17], where even though large (13microns) devices had the highest peak power conversion efficiency, they were outperformed by smaller devices (with lower peak power conversion efficiency) in terms of the maximum lasing temperature (~40 deg C for 13micron apertures versus ~60 deg C for 6micron apertures). Finally, it should be mentioned that CW lasing of 688nm was demonstrated up to 115 deg C [23].

3. ARRAY FABRICATION AND RESULTS

As with high-power 808nm, in the case of 6xx nm VCSEL arrays, the GaAs substrate needs to be removed for efficient heat removal [29]. The processing sequence for high-power red VCSEL arrays is summarized as follows.

First, the epitaxial side of the sample is fully processed, following a sequence similar to that of single devices, with added electro-plated Gold to improve current distribution (Fig. 4(a)).

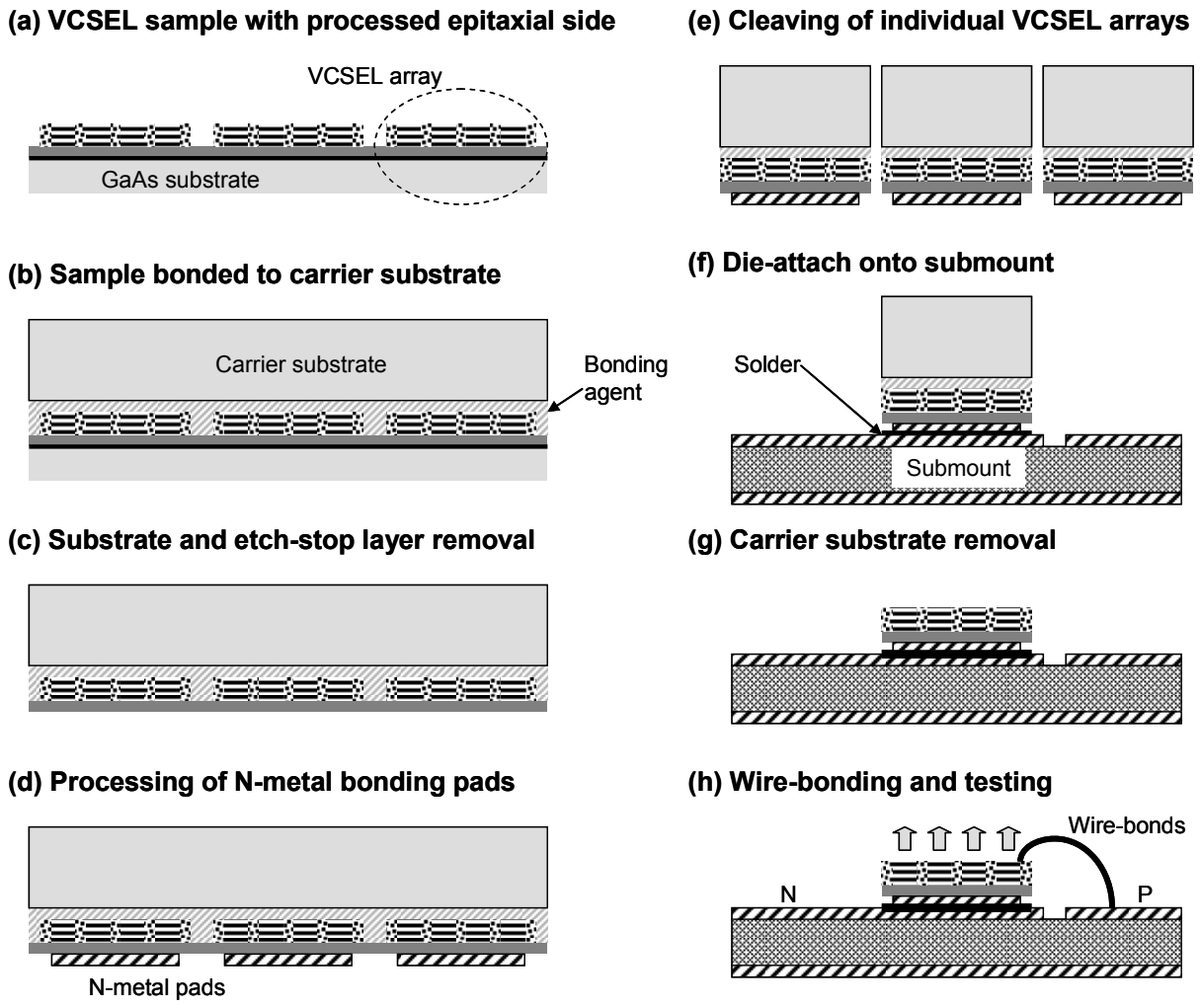

Fig. 4. Processing and packaging steps for red VCSEL arrays. The chip soldered on the submount is only 10microns thick.

Then, the process continues with the following steps (Fig. 4):

(b) The sample, with the epitaxial side fully processed (step (a) – see also Fig. 5), is bonded onto a sacrificial carrier using a special bonding agent.

(c) The GaAs substrate is removed using a selective wet-etch. The etch-stop layer is then removed using another selective wet-etch, thus exposing the N+ GaAs contact layer. At this stage, the sample is only 10microns thick.

(d) Patterned N-metal pads are evaporated onto the N+ GaAs contact layer. Alloying temperature is minimized to avoid affecting the bonding agent, while still providing an Ohmic contact. These bonding pads are then plated with Gold.

(e) The individual arrays are cleaved. Each array is still attached to its individual sacrificial carrier.

(f) Each array/carrier assembly is then soldered to a high-conductivity submount (such as diamond).

(g) The sacrificial carrier is removed and the array-on-submount assembly is cleaned

(h) The array is wire-bonded and tested.

Even though the chips are very thin (10microns), we successfully soldered them on diamond submounts. The chip-on-submount is then mounted on a Copper carrier with leads for testing.

Figure 5 shows a photograph of a packaged red VCSEL array chip on diamond submount as well as a schematic of the cross section of the array mounted on submount.

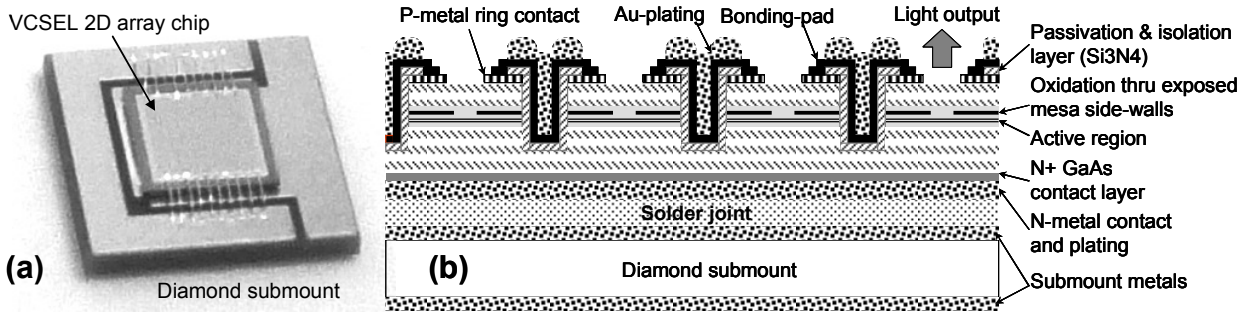

Fig. 5. (a) Photograph of a packaged red VCSEL array chip on diamond submount, and (b) schematic of cross section of array chip on submount.

Figure 6 shows the power versus current and emission spectrum for a 2mm x 2mm 688nm VCSEL array packaged on diamond submount and operated under CW. These arrays contain several hundreds of elements driven in parallel. The LI curves were measured at heat-sink temperatures of 20, 30, 40, and 50 deg C. For each curve, the peak power conversion efficiency point and value are shown. At 20 deg C, a peak efficiency of 22.2% at ~3W output power is demonstrated. The peak efficiency point seems to be at a constant operating current (5A) for the range of temperatures considered, and decreases down to 15.2% at 50 deg C. The emission spectrum is shown at 20 deg C and 5A operating current (Fig. 6(b)). The spectral FWHM is only 0.65nm.

Figure 7 shows the power versus current for larger 4mm x 4mm 650nm and 688nm VCSEL arrays packaged on diamond submount and operated under various duty cycles at a 20 deg C heat-sink temperature. These arrays contain thousands of elements packed more densely than for the 2mm array configuration. The 650nm VCSEL array was operated under a 100micro-second pulse width and duty cycles of 1%, 10%, and 50%. As can be seen, the drop in output power with increasing duty cycle is severe. The array did not lase under CW operation. Under 100us/1% operation at a peak power of ~17W is obtained.

The 688nm 4mm array (Fig. 7(b)) does lase under CW operation, but with a maximum 3.8W output power only. Under 100us/1% QCW operation, the array reaches a peak power of 55W.

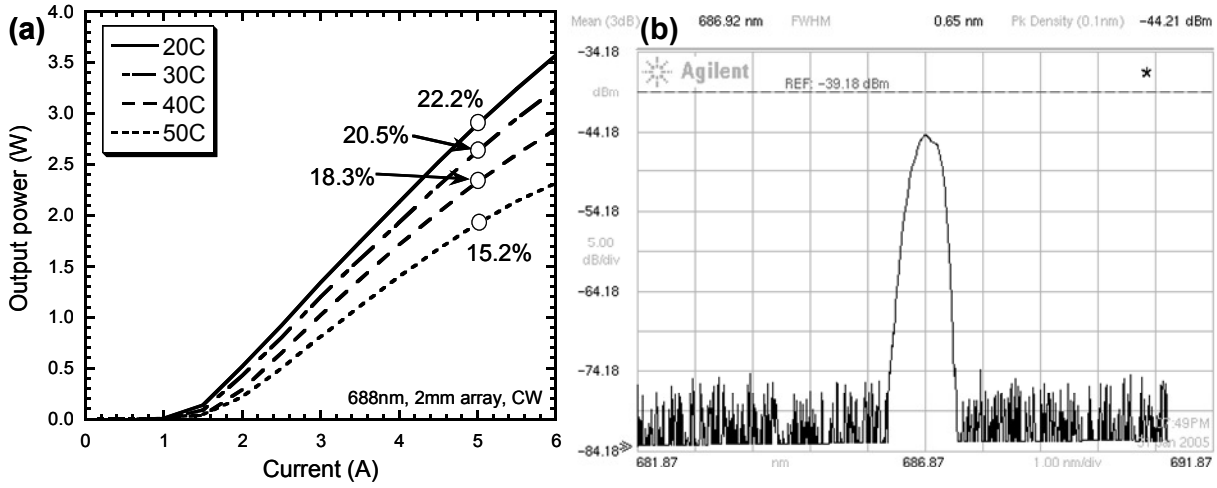

Fig. 6. (a) Output power versus drive current at different heat-sink temperatures of a 2mm x 2mm VCSEL array packaged on diamond submount and emitting around 688nm. The peak power conversion efficiency points are also indicated. (b) Output spectrum at 5A and 20 deg C heat-sink temperature.

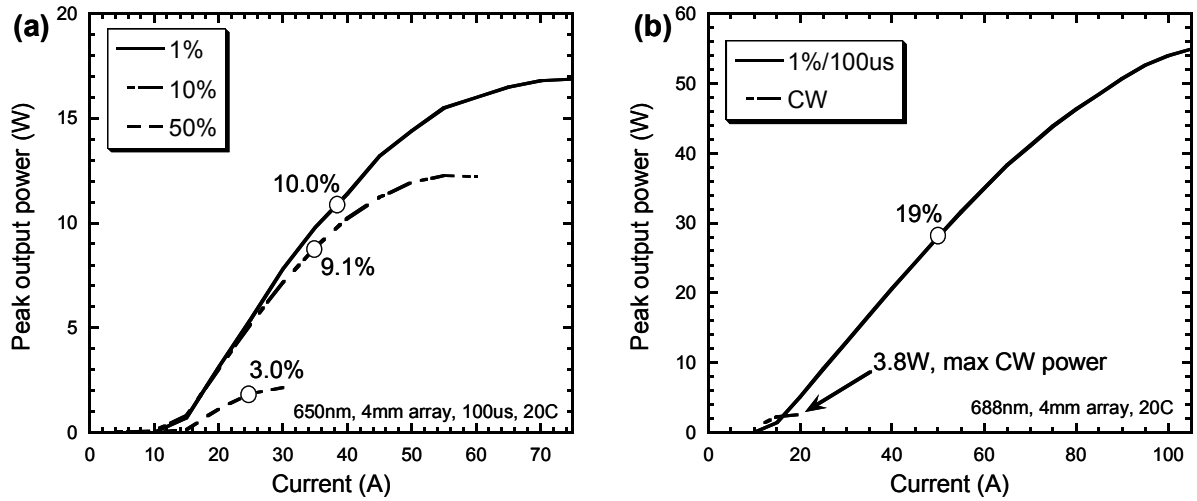

Fig. 7. Output power versus drive current under different driving conditions for two 4mm x 4mm red VCSEL arrays emitting at (a) 650nm and (b) 688nm. The arrays are operated at a 20 deg C heat-sink temperature. The peak power conversion efficiency points are also indicated.

The sub-par CW performance of the 4mm arrays compared to 2mm arrays (and compared to even larger arrays at longer wavelengths such as 808nm and 976nm) highlight the performance sensitivity of these types of material to higher temperature operation. The higher number of elements and higher packing density of the 4mm arrays result in a higher effective junction temperature due to a 'nearest neighbor' effect. Clearly further optimization of the layout and array size is required to improve the CW output power or red VCSEL arrays.

4. SUMMARY

Red VCSELs were developed at the 650nm and 688nm wavelengths, with the aim to develop high-power red laser sources for a variety of applications. Single device performance shows power conversion efficiencies of ~17% for the 650nm wavelength and ~30% for the 688nm, similar to other published results. Large 2D arrays were fabricated by removing the GaAs substrate and mounting the remaining epitaxy on high thermal conductivity diamond submounts. For 2mm x 2mm 688nm VCSEL arrays, 3W output power was demonstrated under CW operation, with a power conversion efficiency of 22.2%. However, for larger, more dense arrays (4mm x 4mm, few thousand elements), CW operation becomes challenging, especially at the shorter, 650nm wavelength. Nevertheless, output powers of 17W (650nm) and 55W (688nm) were obtained under QCW operation at a 20 deg C heat-sink operation. More work is needed to improve the efficiency and temperature performance of these devices (especially at the lower red wavelengths), as well as the designs of the array layouts.

ACKNOWLEDGMENTS

We would like to thank Dr. Tong Chen for help in characterizing some of these red VCSEL arrays.

REFERENCES

[1] Hino, I., Gomyo, A., Kobayashi, K., Suzuki, T., Nishida, K., "Room-temperature pulsed operation of AlGaInP/GaInP/AlGaInP double heterostructure visible light laser diodes grown by metalorganic chemical vapor deposition," Appl. Phys. Lett. **43**(11), 987-989 (1983).

[2] Horiguchi, M., Yoshino, K., Shimizu, M., and Yamada, M., "670nm semiconductor laser diode pumped erbium-doped fiber amplifier," Electron. Lett. **29**(7), 593-595 (1993).

[3] Tsunekane, M., Ihara, M., Taguchi, N., and Inaba, H., "Analysis and design of widely tunable diode-pumped Cr:LiSAF lasers with external grating feedback." IEEE J. Quantum Electron. **34**(7), 1288-1296 (1998).

[4] Charamisinau, I., Happawana, G., S., Evans, G., A., Kirk, J., B., Bour, D., P., Rosen, A., Hsi, R., A., "High-power semiconductor red laser arrays for use in photodynamic therapy," IEEE J. Selected Topics Quantum Electron. **11**(4), 881-891 (2005).

[5] Blume, G., Feise, D., Kaspari, C., Sahm, A., and Paschke, K., "High luminance tapered diode lasers for flying-spot display applications," Proc. SPIE **8280**, 82800E (2012).

[6] Chung, H., Dai, T., Sharma, S., K., Huang, Y.-Y., Carroll, J., D., Hamblin, M., R., "The nuts and bolts of low-level laser (Light) therapy," Annals of Biomedical Engineering **40**(2), 516-533 (2012).

[7] Udrea, M., V., Nica, A., S., Florian, M., Poenaru, D., Udrea, G., Lungeanu, M., Sporea, D., G., Vasiliu, V., V., and Vieru, R., "Diode laser based therapy device," Proc. SPIE **5581**, 677-681 (2004).

[8] Schweizer, H., Ballman, T., Butendeich, R., Rossbach, R., Raabe, B., Jettter, M., and Scholz, F., "Red surface emitters: powerful and fast," Proc. SPIE **5248**, 103-116 (2003).

[9] Kahle, H., Schwarzback, T., Eichfelder, M., Robach, R., Jetter, M., and Michler, P.. "UV laser emission around 330nm via intracavity frequency doubling of a tunable red AlGaInP-VECSEL," Proc. SPIE **8242**, 82420M (2012).

[10] Schneider, R., P., Bryan, R., P., Lott, J., A., and Olbright, G., R., "Visible (657nm) InGaP/InAlGaP strained quantum-well vertical-cavity surface-emitting laser," Appl. Phys. Lett. **60**(15), 1830-1832 (1992).

[11] Schneider, R., P., and Lott, J., A., "Cavity design for improved electrical injection in InAlGaP/AlGaAs visible (639–661 nm) vertical cavity surface emitting laser diodes," Appl. Phys. Lett. **63**(7), 917-919 (1993).

[12] Huang, K., F., Tai, K., Wu, C., C., and Wynn, J., D., "Continuous wave visible InGaP/InGaAlP quantum well surface emitting laser diodes," IEEE Proc. LEOS, 613-614 (1993).

[13] Wilmsen, C., Temkin, H., Coldren, L., A., *Ed.*, [Vertical-Cavity Surface-Emitting Lasers: Design, Fabrication, and Applications], Cambridge University Press, Cambridge, UK (2001).

[14] Michalzik, R., *Ed.*, [VCSELs: Fundamentals, Technology and Applications of Vertical-Cavity Surface-Emitting Lasers], Springer-Verlag, Berlin & Heidelberg (2013).

[15] Choquette, K., D., Schneider, R., P., Crawford, M., H., Geib, K., M., Figiel, J., J., "Continuous wave operation of 640-660 nm selectively oxidized AlGaInP vertical-cavity lasers," Electron. Lett. **31**(14), 1145-1146 (1995).

[16] Knigge, A., Zorn, M., Wenzel, H., Weyers, M., and Trankle, C., "High efficiency AlGaInP-based 650nm vertical cavity surface-emitting lasers," Electron. Lett. **37**(20), 1222–1223 (2001).

[17] Knigge, A., Zorn, M., Sebastian, J., Vogel, K., Wenzel, H., Weyers, M., and Trankle, G., "High-efficiency AIGalnP/AIGaAs vertical-cavity surface-emitting lasers with 650nm wavelength," IEE Proc. **150**(2), 110-114 (2003).

[18] Schweizer, H., Ballmann, T., Butendeich, R., Rossbach, R., Raabe, B., Jetter, M., and Scholz, F., "Red surface emitters: Powerful and fast," Proc. SPIE **5248**, 103-116 (2003).

[19] Rossbach, R., Ballmann, T., Butendeich, R., Schweizer, H., Scholz, F., and Jetter, M., "Red VCSEL for high-temperature applications," J. Crystal Growth **272**(1), 549-554 (2004).

[20] Sale, T., E., Lancefield, D., Corbett, B., Kearney, I., and Justice, J., "Advances in red-emitting VCSELs for polymer fibre applications," Proc. SPIE **5364**, 130-137 (2004).

[21] Duggan, G., D., Barrow, D., A., Calvert, T., Maute, M., Hung, V., McGarvey, B., Lambkin, J., D., and Wipiejewski, T., "Red vertical cavity surface emitting lasers (VCSELs) for consumer applications," Proc. SPIE **6908**, 69080G (2008).

[22] Ohgoh, T., Mukai, A. ,Mukaiyama, A., Asano, H., and Hayakawa, T., "Highly Reliable Operation of Red Laser Diodes for POF Data Links," Electron. & Comm. in Japan **92**(12), 13-19 (2009).

[23] Johnson, K., Hibbs-Brenner, M., Hogan, W., Dummer, M., "Advances in Red VCSEL Technology," Advances in Optical Technologies **2012**, 569379 (2012).

[24] Czyszanowski, T., Sarzała, R., P., Piskorski, L., Dems, M., Wasiak, M., Nakwaski, W., and Panajotov, K., "Comparison of usability of oxide apertures and photonic crystals used to create radial optical confinements in 650-nm GaInP VCSELs," IEEE J. Quantum Electron. **43**(11), 1041-1047 (2007).

[25] Eichfelder, M., Schulz, W.-M., Reischle, M., Wiesner, M., Rossbach, R., Jetter, M., and Michler, P., "Growth and characterization of electrically pumped red-emitting VCSEL with embedded InP/AlGaInP quantum dots," J. Crystal Growth **315**(1), 131-133 (2011).

[26] Schwarzbäck, T., Kahle, H., Eichfelder, M., Roßbach, R., Jetter, M., "Wavelength tunable ultraviolet laser emission via intra-cavity frequency doubling of an AlGaInP vertical external-cavity surface-emitting laser down to 328nm," Appl. Phys. Lett. **99**(26), 261101-2611013 (2011).

[27] Schwarzbäck, T., Eichfelder, M., Schulz, W.-M., Robach, R., Jetter, M., and Michler, P., "Short wavelength red-emitting AlGaInP-VECSEL exceeds 1.2W continuous-wave output power," Appl. Phys. B: Lasers and Optics **102**(4), 789-794 (2011).

[28] Seurin, J. F., Ghosh, C. L., Khalfin, V., Miglo, A., Xu, G., Wynn, J. D., Pradhan, P. and D'Asaro, L. A., "High-power high-efficiency 2D VCSEL arrays," Proc. SPIE **6908**, 690808 (2008).

[29] Seurin, J. F., Xu, G., Khalfin, V., Miglo, A., Wynn, J. D., Pradhan, P., Ghosh, C. L., and D'Asaro, L. A., "Progress in high-power high-efficiency VCSEL arrays," Proc. SPIE **7229**, 722903 (2009).

[30] Coldren, L., A., and Corzine, S., W., [Diode Lasers and Photonic Integrated Circuits], John Wiley & Sons, New York (1995).